Published in final edited form as:
Biochem J. 2013 January 1; 449(1): 61–68. doi:10.1042/BJ20121072.

Reversal of Ion Charge Selectivity Renders the Pentameric Ligand-Gated Ion Channel GLIC Insensitive to Anesthetics

Tommy Tillman[*], **Mary H. Cheng**[*,§], **Qiang Chen**[*], **Pei Tang**[*,‡,§], and **Yan Xu**[*,‡,†]

[*]Department of Anesthesiology, University of Pittsburgh, Pittsburgh, PA 15261

[‡]Department of Pharmacology and Chemical Biology, University of Pittsburgh, Pittsburgh, PA 15261

[§]Department of Computational and System Biology, University of Pittsburgh, Pittsburgh, PA 15261

[†]Department of Structural Biology, University of Pittsburgh, Pittsburgh, PA 15261

Abstract

Pentameric ligand gated ion channels (pLGICs) are a family of structurally homologous cationic and anionic channels involved in neurotransmission. Cationic members of the pLGIC family are typically inhibited by general anesthetics, while anionic members are potentiated. GLIC is a prokaryotic cationic pLGIC and can be inhibited by clinical concentrations of general anesthetics. The introduction of three mutations, Y221A (Y–3′A), E222P (E–2′P) and N224R (N0′R), at the selectivity filter and one, A237T (A13′T), at the hydrophobic gate, converted GLIC to an anion channel. The mutated GLIC (GLIC4) became insensitive to the anesthetics propofol and etomidate as well as the channel blocker picrotoxin. Molecular dynamics (MD) simulations revealed changes in the structure and dynamics of GLIC4 in comparison to GLIC, particularly in the tilting angles of the pore-lining helix (TM2) that consequently resulted in different pore radius and hydration profiles. Propofol binding to an intra-subunit site of GLIC shifted the tilting angles of TM2 towards closure at the hydrophobic gate region, consistent with propofol inhibition of GLIC. In contrast, the pore of GLIC4 was much more resilient to perturbation from propofol binding. This study underscores the importance of pore dynamics and conformation to anesthetic effects on channel functions.

Keywords

GLIC; ion selectivity; anesthetic action; pentameric ligand-gated ion channels (pLGICs)

To whom correspondence should be addressed: Yan Xu, Departments of Anesthesiology, Pharmacology and Chemical Biology, and Structural Biology, University of Pittsburgh, Pittsburgh, PA 15261, University of Pittsburgh School of Medicine, 2048 Biomedical Science Tower 3, 3501 Fifth Avenue, Pittsburgh, PA 15260, USA, Tel.:(412) 648-9922, Fax: (412) 648-8998, xuy@anes.upmc.edu; or Pei Tang, Departments of Anesthesiology, Pharmacology & Chemical Biology, and Computational and System Biology, University of Pittsburgh School of Medicine, 2049 Biomedical Science Tower 3, 3501 Fifth Avenue, Pittsburgh, PA 15260, USA, Tel.:(412) 383-9798, Fax: (412) 648-8998, tangp@anes.upmc.edu.

INTRODUCTION

An intriguing relationship exists between ion charge selectivity and anesthetic response in members of the pentameric ligand-gated ion channel (pLGIC)[1] family, which includes both cation channels such as the nicotinic acetylcholine receptors (nAChRs) and serotonin (5-HT_3) receptors, and anion channels such as the $GABA_A$ and glycine receptors. These channels are involved in neurotransmission and respond to clinical concentrations of anesthetics. However, their responses to anesthetics vary significantly depending on their ion charge selectivity. In spite of some exceptions, cationic members are generally inhibited by general anesthetics, while anionic members are potentiated [1, 2].

Although the molecular mechanism of anesthetic action on pLGICs is not fully understood, much progress has been made recently, including the successful crystallization of GLIC, a proton-gated cationic pLGIC from *Gloeobacter violaceus*, in complex with the general anesthetics propofol and desflurane [3]. GLIC shares certain pharmacological properties with eukaryotic cation pLGICs and is inhibited by general anesthetics at concentrations comparable to those inhibiting eukaryotic members of the pLGIC family [4]. Crystal structures of propofol and desflurane bound GLIC reveal an intra-subunit anesthetic binding pocket, which is located in the upper part of the transmembrane helices (TM1-TM4) of each subunit [3]. The identified binding pocket is just on the other side of the pore-lining TM2 and behind the hydrophobic gate of the pore. The binding pocket identified in GLIC may also exist in eukaryotic pLGICs [5-9], though the size and shape probably vary in individual channels. Nevertheless, available structural and functional information has made GLIC invaluable for the understanding of allosteric anesthetic action on pLGICs.

Eukaryotic and prokaryotic pLGICs share the same general structure features, comprising homo- or hetero- pentameric complexes. Each subunit contains a ligand-binding extracellular domain, a transmembrane pore, and an optional cytoplasmic domain. Ion charge selectivity is determined by the transmembrane pore [10]. It was first demonstrated in the homomeric α7 nAChR [11] that mutagenesis of the pore region can interconvert cation channels to anion channels. A minimal number of mutations, including replacing the glutamate at the -1′ position in TM2 with an alanine and introducing a proline at the -2′ position, was sufficient to reverse the ion charge selectivity of the α7 nAChR. An additional V13′T mutation was necessary to have significant conductance of anions, though that mutation did not, by itself, reverse ion selectivity. Similar results were obtained by mutagenesis of the cationic 5-HT3 receptor [12]. The reverse was also true; the anionic glycine and GABA receptors could be converted to robust cation channels by introduction of glutamate at the -1′ position and the removal of proline at the -2′ position [13-16]. These findings on eukaryotic pLGICs established a basis for reversing the ion charge selectivity of GLIC with minimal mutations. The anesthetic response of these ion charge reversal mutants has not been reported. GLIC and its anion-conducting mutant would form a valuable pair for elucidating the determinant(s) of anesthetic inhibition or potentiation.

[1]The abbreviations used are:
pLGIC, pentameric ligand gated ion channel; nAChRs, nicotinic acetylcholine receptors; TM1-4, transmembrane helix 1 through 4, PMF, potential of mean force; MD, molecular dynamic; ABF, adaptive biasing force; RMSF, root mean-square fluctuations; GluCl , glutamate-gated chloride channel from *Caenorhabditis elegans*; GABAR, GABA receptor; GlyR, glycine receptor.

Here we explore the relationship between ion charge selectivity and anesthetic response in GLIC. GLIC was changed from a cation channel to an anion channel with only three mutations at the selectivity filter (Y–3′A, E–2′P, N0′R) and one at the hydrophobic gate (A13′T). The mutations changed not only the channel ion charge selectivity, but also the channel responses to general anesthetics. The mutated channel, GLIC4, became much less sensitive to anesthetics than GLIC in electrophysiology measurements. These experimental studies were complemented by computational efforts. Our calculations of potential of mean force (PMF) revealed changes between GLIC and GLIC4 in the energy landscape for Cl^- permeation. Molecular dynamic (MD) simulations elucidated potential structural and dynamical causes of anesthetic insensitivity in GLIC4. Altogether, our functional and computational investigations on GLIC4, in combination with previous characterizations of GLIC, provide compelling evidence that subtle changes in the pore can generate distinctly different responses to anesthetic modulation.

EXPERIMENTAL

Mutagenesis and functional measurements

pTLN-GLIC for expression of GLIC in Xenopus oocytes was generously provided by Professor Raimund Dutzler's group of the University of Zürich, Switzerland. All mutagenesis was done using the Quickchange Lightning Mutagenesis Kit (Agilent) and confirmed by sequencing. Capped complementary RNA was synthesized with the mMessage mMachine Sp6 kit (Ambion), purified with the RNeasy kit (Qiagen), and 25-50 ng injected into *Xenopus laevis* stage 5-6 oocytes. Oocytes were maintained at 18 °C in modified Barth's saline [17]. Two-electrode voltage clamp experiments were performed at room temperature 16-48 hrs after injection with a model OC-725C amplifier (Warner Instruments), and a 20 μl oocyte recording chamber (Automate Scientific). Oocytes were clamped to a holding potential of –40 to -60 mV. Currents were recorded in ND-96 [18] supplemented with 10 mM MES and adjusted to the indicated pH. Ion selectivity experiments were performed using a buffer consisting of 10 mM HEPES, 10 mM MES, 2 mM $CaSO_4$, 130 mM NaCl with choline substituted for sodium and gluconate substituted for chloride, and pH was adjusted using choline hydroxide and gluconic acid. Data were collected and processed using Clampex 10 (Molecular Devices). Non-linear regressions were performed using Igor Pro (Wavemetrics) and Prism (Graphpad) software.

Molecular dynamics and docking analysis

For MD simulation, five systems were constructed using VMD [19]: (1) GLIC (PDB: 3EAM); (2) GLIC4, which resulted from in silico mutations on GLIC that include Y–3′A, E–2′P, N0′R, and A13′T; (3) GLIC3, which is the same as GLIC4 but without A13′T mutation; (4) GLIC-PFL, in which propofol molecules were bound to two consecutive intra-subunit anesthetic binding sites identified in the GLIC structure [3]; and (5) GLIC4-PFL, in which propofol molecules were bound to the same sites as in GLIC-PFL. The choice of two propofol molecules for systems GLIC-PFL and GLIC4-PFL was on the basis of our simulation studies, in which we found that symmetrically bound propofol, as shown in the crystal structure [3], stabilized the open channel conformation of GLIC, while asymmetrically bound propofol facilitated the transition of the channel from an open to a

closed conformation (unpublished data). The simulations suggest that two or three propofol binding resembles better the propofol inhibition effect on GLIC. The protein in each system was inserted into the center of a cylinder of preequilibrated POPE/POPG (3:1) binary lipid mixture [20]. MD simulations were carried out using the NAMD2 program [21] and CHARMM27 force field with CMAP corrections (version 31) [22]. No constraint was placed on protein, lipids, or propofol in simulations after the initial 2.5 ns equilibration. The single ion potential of mean forces (PMFs) for transporting a Na^+ or Cl^- ion through the GLIC or GLIC4 channel were calculated using the adaptive biasing force (ABF) [23, 24] method implemented in NAMD. The same calculation protocol reported previously was used [25]. Picrotoxin binding sites were predicted based on flexible docking using the Autodock program [26] (version 3.0.05). For systems GLIC, GLIC4, GLIC-PFL, GLIC4-PFL, each had 3 replicate MD simulations. Each simulation lasted for 50 ns.

RESULTS

Mutations in the selectivity filter and hydrophobic gate convert GLIC to a Cl^- channel

In most cationic members of the pLGIC family, the selectivity filter consists of the canonical arginine or lysine at position $0'$ with a glutamate at position $-1'$. GLIC has an anomalous selectivity filter with an asparagine at position $0'$, and the glutamate shifted to the $-2'$ position. Three mutations were engineered to change the selectivity filter between $-3'$ and $0'$ in GLIC to match that of the glycine receptor, an anionic member of the pLGIC family, to form GLIC3 (Figure 1A, 1B). GLIC3 showed a small but detectable current. A previous anionic conversion of α7 AChR suggested that an additional mutation in the hydrophobic gate region, V13′T, was needed in order to have an adequate channel current [11, 27]. We engineered a similar mutation, A13′T, in the hydrophobic region of GLIC3 to make GLIC4 (Figure 1A, 1B). GLIC is a proton gated channel, with the EC_{50} at pH 5. GLIC4 achieved current amplitudes comparable to wild type GLIC, though with a shift in the EC_{50} from pH 5 to pH 4.3 (Figure 1C).

Given the close proximity of the A13′T to the intra-subunit anesthetic binding site, we also engineered a construct with only the A13′T mutation, GLICT (Figure 1A, 1B). This construct had an EC_{50} at pH 5.9 that was decreased almost an order of magnitude relative to GLIC (Figure 1C). This is similar to what was seen for α7 AChR, where a comparable mutation reduced the agonist concentration at the EC_{50} over two orders of magnitude [11].

Reversal-potential measurements in *Xenopus* oocytes expressing GLIC4 and GLICT revealed that GLIC4, but not GLICT, had become anion selective, with a 18-fold preference for Cl^- ions over Na^+ ions (Figure 2). For GLIC4, replacing sodium in the external buffer with choline showed no effect on the reversal potential, but replacing chloride with gluconate showed a 60 mV positive shift in the reversal potential, indicative of chloride selectivity. The IV curves were fit directly to the Goldman-Hodgkin-Katz equation to estimate the permeability ratio $P_{Cl}/P_{Na}=18\pm5$ (Figure 2A). In contrast, for GLICT, there was no change in reversal potential replacing chloride ion (Figure 2B). A negative shift in reversal potential upon replacing sodium with choline indicated that GLICT remained sodium selective.

The ion charge reversal mutant, GLIC4, is insensitive to anesthetics

The general anesthetics propofol and etomidate inhibit most cationic members and potentiate most anionic members of the pLGIC family [2]. As a cation channel, GLIC is inhibited by both anesthetics (Figure 3). GLICT showed only a small change in its sensitivity to propofol and a modest change in its sensitivity to etomidate. In contrast, GLIC4 was almost insensitive to inhibition by propofol and etomidate (Figure 3). The effect of propofol inhibition was quantified in Figure 4. The half-maximal inhibitory concentration (IC_{50}) of propofol was measured at the EC_{20} of the pH dependent activation for each construct, showing less than a 2-fold decrease in anesthetic sensitivity for GLICT, but a close to 30-fold decrease in sensitivity for GLIC4. Such a distinct difference highlights the importance of the mutations at the selectivity filter of GLIC4 in anesthetic action.

Pore profile changes in GLIC4

To elucidate channel structural and dynamic differences that may be responsible for functional changes, we performed *in silico* mutations on the GLIC structure [28] matching our experimental design. Well-equilibrated structures of GLIC4 were obtained via subsequent MD simulations, as evident in plateau of backbone root mean square deviation (Figure S1) and stable pore radius profiles (Figure S2) (see details in supporting information). In comparison with GLIC, several changes in GLIC4 are notable and functionally relevant.

Potential of mean force (PMF) calculations echo the experimental finding that GLIC4 is highly permeable to Cl^- but not Na^+. As shown in Figure 5, mutations at the selectivity filter reshaped PMF profiles of a single Na^+ or Cl^- passing through the GLIC4 channel. The PMF for Cl^- changed from a significant energy barrier in GLIC to an energy well in GLIC4 near the selectivity filter. The PMF for Na^+, however, changed oppositely. Compared to GLIC3 (without the A13′T mutation), a smaller PMF was observed in GLIC4 near A13′T that could account for the larger current observed in GLIC4 (Figure S3).

Despite an overall structural similarity of GLIC and GLIC4, structural deviations of GLIC4 from GLIC, especially in the mutated selectivity filter region, were evident. In all three runs of parallel simulations, GLIC4 developed an enlarged pore radius at the selectivity filter and a decreased pore radius at the hydrophobic gate (Figure 6A). The radial tilting angle of the TM2 helix reduced 2–3° in GLIC4 relative to GLIC (Figure 6B). Such a deviation of the pore profile would predict consequences on picrotoxin binding, which was suggested to be near the selectivity filter inside the pore of GLIC [29]. Indeed, we found picrotoxin docked well in that region of GLIC, but picrotoxin did not dock near the selectivity filter in GLIC4, presumably due to a larger pore radius. In addition, our electrophysiology measurements showed picrotoxin inhibition in *Xenopus* oocytes expressing GLIC and GLICT, but no effect in those expressing GLIC4 under the same conditions (Figure S4). Taken together, these results support the notion that the pore geometry of GLIC4 deviated from GLIC.

The mutations also altered the mobility of the selectivity filter and the hydrophobic gate inside the pore. Root mean-square fluctuations (RMSF) of the Cα atoms in the TM1-2 linker and the selectivity filter of the pore were much higher in GLIC4 than GLIC, signing

increased motion in that region of GLIC4 (Figure S5). Increased flexibility of the selectivity filter region may have also contributed to the change of picrotoxin binding in GLIC4. The RMSF near the middle section of TM2, however, were decreased in GLIC4, indicative of a rigidified hydrophobic gate. RMSF in other regions of the TM domains were more or less the same in GLIC and GLIC4. Changes in RMSF of GLIC4 are consistent with the observed changes in pore profile: an expanded pore radius near the selectivity filter and a shrunken pore radius at the hydrophobic gate.

GLIC4 had a pore hydration profile distinct from GLIC. Histograms of water in the hydrophobic gate region (9′-16′) were generated from three replicate 50-ns simulations for each system (Figure 7). Functional measurements show that at pH 4.6, GLIC and GLIC4 have ~73% and ~21% of the maximum current, respectively. Consistent with the experimental data, our simulations at pH 4.6 also show hydrated pores of GLIC4 and GLIC for most of the time of the simulations. However, it is notable in the absence of propofol (Figure 7) that GLIC has more water around the hydrophobic gate (9′-16′) than GLIC4, but also shows a small population with a dehydrated pore. Conversely, GLIC4 has less water at the hydrophobic gate, probably due to a narrower pore in the region, but the A13′T mutation prevents the region from complete drying. Mutations at the selectivity filter of GLIC4 increased the first and second hydration shells of Cl^- ions at the selectivity filter up to 8% and 20%, respectively (Figure S6).

Propofol binding accelerates the closing of GLIC, but not GLIC4, in MD simulations

To understand why GLIC4 is virtually insensitive to anesthetics, we performed MD simulations on both GLIC4 and GLIC in the presence of propofol, which was bound to the site identified in the crystal structure of the GLIC-propofol complex [3]. As shown in Figure 7, propofol binding dramatically decreased hydration of this region in GLIC, while it had only a minor impact to the same region in GLIC4. The stable hydration status of the pore in GLIC4 may have contributed to the insensitivity of GLIC4 currents to propofol binding. Another distinction between GLIC4 and GLIC that potentially relates to the anesthetic insensitivity of GLIC4 lies in the orientation of the pore-lining helix, which is described by radial and lateral tilting angles [20]. Histograms of TM2 helical tilting angles of GLIC and GLIC4 demonstrate obvious differences (Figure S7). The most distinct difference is that upon propofol binding, the distribution range of tilting angles increased profoundly in GLIC, but decreased in GLIC4. In other words, propofol increased conformational heterogeneity in GLIC, but had an opposite effect on GLIC4. The shift direction of tilting angles after adding propofol is also worth noting. In the absence of propofol, GLIC has the highest population of radial and lateral tilting angles of 6° and -0.5°, respectively, which correspond to an open channel conformation [28, 30]. Adding propofol to GLIC generated a new population of radial and lateral tilting angles that moved to the direction favorable for a closed channel conformation [31]. In contrast, adding propofol to GLIC4 did not produce a new population of tilting angles and the conformational redistribution upon propofol binding occurred only within the range of tilting angles in the absence of propofol.

DISCUSSION

Although GLIC is a proton-gated channel, its requirement for ion charge selectivity reversal is virtually the same as that of eukaryotic pLGICs, suggesting a universal pattern of residues responsible for ion charge selectivity in pLGICs. Three mutations at the selectivity filter (Y–3′A, E–2′P, N0′R) and one at the hydrophobic gate (A13′T) in GLIC4 produced a robust anionic current with a shift in EC_{50} towards a higher ligand (proton) concentration. Similar results were observed previously for eukaryotic pLGICs. The A13′T mutation in GLIC4 is comparable to the V13′T mutations required for ion selectivity reversal in the eukaryotic cation channels, nAChR and 5HT3A receptor [11, 12]. Other ion reversal mutants in the pLGIC family also showed changes in the EC_{50} for their respective ligands; a decrease for the α7 nAChR and 5HT3A receptors [11, 12, 27, 32], and an increase for the GABA and glycine receptors [15, 33]. Given that the minimal mutations for ion charge reversal are similar for the cation channels GLIC, nAChR and 5HT3A, the GLIC4 structure may reflect the structural features of the charge-reversal mutants for nAChRs and 5HT3A receptors that have been largely unknown in the past.

The A13′T mutation was necessary for substantial conductance, but the mutations at the selectivity filter had already significantly reduced the energy barrier for chloride ion permeability at both the selectivity filter and the hydrophobic gate (compare Figure 5 and Figure S3). Changes in electrostatics at the selectivity filter (the E–2′P, N0′R mutations) have an obvious role in ion charge selectivity. In addition, changes in the dynamics and tilting angles of TM2 as well as the radius and hydration profiles of the pore may affect ion charge selectivity reversal in GLIC4. Previous studies also observed a link between ion charge selectivity and pore radius or hydration profiles for the glycine receptor [13, 14] and GLIC [25, 34]. The most significant barrier for Cl^- in GLIC is located at the selectivity filter at the intracellular end of the pore, due to the funnel shape of the pore and a strong unfavorable interaction with E−2′ [25, 34]. In GLIC4, the unfavorable interaction is replaced with a favorable interaction for Cl^- (N0′R). Furthermore, an enlarged pore at the selectivity filter region significantly reduced the dehydration energy barrier for Cl^- transport. Both changes benefit Cl^- conduction.

The observed pore widening at the selectivity filter in GLIC4 has not been reported previously. The only X-ray structure for a native anionic pLGIC is the glutamate-gated chloride channel from the nematode *Caenorhabditis elegans* (GluCl), which shows a pore profile similar to that of GLIC [7]. The smallest pore radius (2.3 Å) of GluCl is at P–2′ in the selectivity filter [7]. In GLIC4, however, the TM2 helix is tilted away from the pore at P–2′, yielding a radius of 3.6 Å at the intracellular end of the pore. The functional constriction of the pore radius in GLIC4 is apparently located at the hydrophobic gate, but the A13′T mutation reduced the hydrophobic barrier in this region. Whether the pore arrangement seen in GLIC4 also exists in native members of the pLGIC family will await future structure determinations. It remains a great challenge to capture different functional conformations of a given channel in crystallography [35]. However, it is encouraging to see that a “locally closed” conformation of GLIC showing closure near the hydrophobic gate region has been captured recently in X-ray structures of GLIC after mutagenesis and cross-linking manipulations [31].

Does the GLIC4 structure represent a native conformation of eukaryotic pLGICs? It seems too early to have a definitive answer before a sufficient number of structures for eukaryotic pLGICs become available. However, one can get a clue through picrotoxin binding. The GluCl structure shows picrotoxin bound between T2′ and P-2′ inside the pore [7]. Mutagenesis data on GLIC also suggest the importance of T2′ to picrotoxin binding [29]. The importance of the intracellular pore entrance to picrotoxin binding is also shown in eukaryotic pLGICs, including cationic α7nAChR and α3β4 nAChR [36] and anionic GlyR [37], $GABA_AR$ [38], and $GABA_CR$ [39]. Picrotoxin is a potent channel blocker for many pLGICs, including a GLIC-GlyR chimera [40]. However, some eukaryotic anionic pLGICs are not sensitive to picrotoxin inhibition. For example, homomeric α GlyRs can be inhibited by picrotoxinin, the most active component of picrotoxin, at low μM concentrations, but heteromeric α/β GlyRs are picrotoxinin-insensitive channels [37]. That is thought to be the reason why no picrotoxin inhibition is seen in adult spinal cord [37]. Heteromeric 5-HT3A/3B receptors are also insensitive to picrotoxin [41]. It seems premature to assume that the pore features of these heteromeric eukaryotic pLGICs resemble those of GLIC4, but GLIC4 does share the common functional state of insensitivity to picrotoxin with these heteromeric eukaryotic pLGICs.

At the pH corresponding to the EC_{20}, GLIC was inhibited by propofol with an IC_{50} of 21 μM, which is similar to the propofol inhibition concentrations observed for eukaryotic pLGICs. For example, the cation channel α4β2 nAChR shows propofol inhibition with an IC_{50} of 4.5–19 μM [42, 43]. In GLIC4, the anionic charge selectivity was accompanied with insensitivity to the anesthetics propofol and etomidate. The absence of anesthetic potentiation effects on GLIC4 is not totally unexpected. Although it is true that general anesthetics inhibit or potentiate most cationic or anionic members of the pLGIC family, respectively, there are notable exceptions. For example, among eukaryotic anionic pLGICs, $GABA_AR$ is potentiated by etomidate, but both α1 and α1β GlyRs are insensitive to etomidate [44]. Between the two mutation sites in GLIC4, which one holds the primary responsibility for the lost of sensitivity to anesthetics? The A13′T site is closer to the intra-subunit anesthetic binding pocket described in the X-ray structure of propofol bound to GLIC [3]. A13′T faces the pore and is just behind the anesthetic binding pocket. However, GLICT, with the single mutation A13′T, remains sensitive to anesthetics. A13′T alone is not sufficient to abolish the anesthetic sensitivity. Mutations to the selectivity filter and subsequent changes in the dynamics and tilting angle of TM2 are essential to the observed changes of anesthetic sensitivity.

It is worth mentioning that unlike the case of propofol, there is no high-resolution structural data to support an etomidate binding site in GLIC. The A13′T mutation in GLICT caused a modest reduction of etomidate inhibition (Figure 3). A similar reduction of picrotoxin inhibition was also observed in GLICT (Figure S4). Thus, our data do not exclude the possibility that etomidate may also act as picrotoxin to block the pore of GLIC. Apparently, further investigation is needed before reaching a solid conclusion.

Our MD simulations showed that propofol binding to GLIC shifted the TM2 tilting angles towards a dehydration conformation at the hydrophobic gate region, but had no such effect on GLIC4. Upon propofol binding to GLIC4, not only did the A13′T mutation protect this

region from dehydration, but also the combined mutations made the GLIC4 conformation insensitive to propofol binding. The resistance of TM2 tilting to propofol binding could also be responsible for the insensitivity of GLIC4 to anesthetics.

The unique TM2 backbone dynamics in GLIC4 may contribute to the channel insensitivity to anesthetic binding. Comparing to the pore lining TM2 in GLIC, both the extracellular and intracellular ends of TM2 in GLIC4 show a higher flexibility, whereas the middle section of TM2 has a slightly increased rigidity (Figure S5). These features can facilitate a rigid body adjustment of the TM2 helix to instantaneously buffer perturbations from anesthetic binding. It was evident in a previous study of GLIC that the size of the pore fluctuated in response to the presence or absence of ions [34]. The pore could dilate temporarily when an ion occupied the pore and revert to the initial size after passage [34]. It was also observed previously that ion translocation through the nAChR channel relied on channel hydration coupled with dynamic fluctuation of the channel structure [45]. GLIC4 possesses more flexibility to adjust the pore size, which can cushion the impact of anesthetic binding, yielding a channel insensitive to anesthetics.

It has been suggested that anesthetics are likely to bind to multiple sites within GLIC [46] in addition to the intra-subunit cavity identified in the X-ray structure [3]. It remains a great challenge to pinpoint which anesthetic sites hold the primary responsibility for functional responses. However, no matter where anesthetics bind to the protein, the response of the transmembrane pore to anesthetic binding ultimately determines the functional consequence. In the case of GLIC and GLIC4, it is likely that they share the same sites for anesthetics. Distinct functional responses to anesthetics between GLIC and GLIC4 result from differences in their pore hydration status, conformation and dynamics. This notion may have general implications, considering that anionic pLGICs have many more hydrophilic residues lining the pore than cationic pLGICs. Further structural and dynamical investigations are needed to understand the mechanism of how pore attributes affect anesthetic response. At present, our study underscores the importance of pore dynamics and conformation to anesthetic effects on channel functions.

Supplementary Material

Refer to Web version on PubMed Central for supplementary material.

Acknowledgments

We thank Edom Seyoum for technical assistance, Dr. Ossama Kashlan for his helpful discussions, and David Mowrey for his analysis of computational results.

FUNDING

This work was supported by National Institutes of Health [R01GM066358, R01GM056257 (PT), and R37GM049202 (YX)]; supported in part by the National Science Foundation through TeraGrid resources [TG-MCB050030N, TG-MCB100047, and TG-MCB100069] that are hosted by Indiana University, LONI, NCAR, NCSA, NICS, ORNL, PSC, Purdue University, SDSC, TACC, and UC/ANL; supported in part by the National Institutes of Health through resources provided by the National Resource for Biomedical Supercomputing (P41 RR06009), which is part of the Pittsburgh Supercomputing Center.

REFERENCES

1. Franks NP, Lieb WR. Molecular and cellular mechanisms of general anaesthesia. Nature. 1994; 367:607–614. [PubMed: 7509043]
2. Dilger JP. The effects of general anaesthetics on ligand-gated ion channels. Br. J. Anaesth. 2002; 89:41–51. [PubMed: 12173240]
3. Nury H, Van Renterghem C, Weng Y, Tran A, Baaden M, Dufresne V, Changeux JP, Sonner JM, Delarue M, Corringer PJ. X-ray structures of general anaesthetics bound to a pentameric ligand-gated ion channel. Nature. 2011; 469:428–431. [PubMed: 21248852]
4. Weng Y, Yang L, Corringer PJ, Sonner JM. Anesthetic sensitivity of the Gloeobacter violaceus proton-gated ion channel. Anesth. Analg. 2010; 110:59–63. [PubMed: 19933531]
5. Bertaccini EJ, Wallner B, Trudell JR, Lindahl E. Modeling anesthetic binding sites within the glycine alpha one receptor based on prokaryotic ion channel templates: the problem with TM4. J. Chem. Inf. Model. 2010; 50:2248–2255. [PubMed: 21117677]
6. Murail S, Wallner B, Trudell JR, Bertaccini E, Lindahl E. Microsecond simulations indicate that ethanol binds between subunits and could stabilize an open-state model of a glycine receptor. Biophys. J. 2011; 100:1642–1650. [PubMed: 21463577]
7. Hibbs RE, Gouaux E. Principles of activation and permeation in an anion-selective Cys-loop receptor. Nature. 2011; 474:54–60. [PubMed: 21572436]
8. Perkins DI, Trudell JR, Asatryan L, Davies DL, Alkana RL. Charge and Geometry of Residues in the Loop 2 beta Hairpin Differentially Affect Agonist and Ethanol Sensitivity in Glycine Receptors. J. Pharmacol. Exp. Ther. 2012; 341:543–551. [PubMed: 22357974]
9. McCracken LM, McCracken ML, Gong DH, Trudell JR, Harris RA. Linking of Glycine Receptor Transmembrane Segments Three and Four Allows Assignment of Intrasubunit-Facing Residues. ACS Chem. Neurosci. 2010; 1:482. [PubMed: 21326622]
10. Keramidas A, Moorhouse AJ, Schofield PR, Barry PH. Ligand-gated ion channels: mechanisms underlying ion selectivity. Prog. Biophys. Mol. Biol. 2004; 86:161–204. [PubMed: 15288758]
11. Galzi JL, Devillers-Thiery A, Hussy N, Bertrand S, Changeux JP, Bertrand D. Mutations in the channel domain of a neuronal nicotinic receptor convert ion selectivity from cationic to anionic. Nature. 1992; 359:500–505. [PubMed: 1383829]
12. Gunthorpe MJ, Lummis SC. Conversion of the ion selectivity of the 5-HT(3a) receptor from cationic to anionic reveals a conserved feature of the ligand-gated ion channel superfamily. J. Biol. Chem. 2001; 276:10977–10983.
13. Lee DJ, Keramidas A, Moorhouse AJ, Schofield PR, Barry PH. The contribution of proline 250 (P-2′) to pore diameter and ion selectivity in the human glycine receptor channel. Neurosci. Lett. 2003; 351:196–200. [PubMed: 14623139]
14. Keramidas A, Moorhouse AJ, Pierce KD, Schofield PR, Barry PH. Cation-selective mutations in the M2 domain of the inhibitory glycine receptor channel reveal determinants of ion-charge selectivity. J. Gen. Physiol. 2002; 119:393–410. [PubMed: 11981020]
15. Wotring VE, Miller TS, Weiss DS. Mutations at the GABA receptor selectivity filter: a possible role for effective charges. J. Physiol. 2003; 548:527–540. [PubMed: 12626678]
16. Jensen ML, Timmermann DB, Johansen TH, Schousboe A, Varming T, Ahring PK. The beta subunit determines the ion selectivity of the GABAA receptor. J. Biol. Chem. 2002; 277:41438–41447. [PubMed: 12177063]
17. Sive, HL.; Grainger, RM.; Harland, RM. Early development of Xenopus laevis : a laboratory manual. Cold Spring Harbor Laboratory Press; Cold Spring Harbor, NY.: 2000.
18. Dascal N. Voltage clamp recordings from Xenopus oocytes. Curr. Protoc. Neurosci. 2001 Chapter 6, Unit 6 12.
19. Humphrey W, Dalke A, Schulten K. VMD: visual molecular dynamics. J. Mol. Graph. 1996; 14:33–38. [PubMed: 8744570]
20. Willenbring D, Liu L, Mowrey D, Xu Y, Tang P. Isoflurane Alters the Structure and Dynamics of GLIC. Biophys. J. 2011; 101:1905–1912. [PubMed: 22004744]

21. Phillips JC, Braun R, Wang W, Gumbart J, Tajkhorshid E, Villa E, Chipot C, Skeel RD, Kale L, Schulten K. Scalable molecular dynamics with NAMD. J. Comput. Chem. 2005; 26:1781–1802. [PubMed: 16222654]
22. MacKerell AD, Bashford D, Bellott M, Dunbrack RL, Evanseck JD, Field MJ, Fischer S, Gao J, Guo H, Ha S, Joseph-McCarthy D, Kuchnir L, Kuczera K, Lau FTK, Mattos C, Michnick S, Ngo T, Nguyen DT, Prodhom B, Reiher WE, Roux B, Schlenkrich M, Smith JC, Stote R, Straub J, Watanabe M, Wiorkiewicz-Kuczera J, Yin D, Karplus M. All-atom empirical potential for molecular modeling and dynamics studies of proteins. J. Phys. Chem. B. 1998; 102:3586–3616.
23. Chipot C, Hénin J. Exploring the free-energy landscape of a short peptide using an average force. J. Chem. Phys. 2005; 123:244906. [PubMed: 16396572]
24. Darve E, Rodriguez-Gomez D, Pohorille A. Adaptive biasing force method for scalar and vector free energy calculations. J. Chem. Phys. 2008; 128:144120. [PubMed: 18412436]
25. Cheng MH, Coalson RD, Tang P. Molecular dynamics and brownian dynamics investigation of ion permeation and anesthetic halothane effects on a proton-gated ion channel. J. Am. Chem. Soc. 2010; 132:16442–16449. [PubMed: 20979415]
26. Morris GM, D.S. G. Halliday RS, Huey R, Hart WE, Belew RK, Olson AJ. Automated docking using a Lamarckian genetic algorithm and an empirical binding free energy function. J. Comput. Chem. 1998; 19:1639–1662.
27. Corringer PJ, Bertrand S, Galzi JL, Devillers-Thiery A, Changeux JP, Bertrand D. Mutational analysis of the charge selectivity filter of the alpha7 nicotinic acetylcholine receptor. Neuron. 1999; 22:831–843. [PubMed: 10230802]
28. Bocquet N, Nury H, Baaden M, Le Poupon C, Changeux JP, Delarue M, Corringer PJ. X-ray structure of a pentameric ligand-gated ion channel in an apparently open conformation. Nature. 2009; 457:111–114. [PubMed: 18987633]
29. Alqazzaz M, Thompson AJ, Price KL, Breitinger HG, Lummis SC. Cys-loop receptor channel blockers also block GLIC. Biophys. J. 2011; 101:2912–2918. [PubMed: 22208189]
30. Hilf RJ, Dutzler R. Structure of a potentially open state of a proton-activated pentameric ligand-gated ion channel. Nature. 2009; 457:115–118. [PubMed: 18987630]
31. Prevost MS, Sauguet L, Nury H, Van Renterghem C, Huon C, Poitevin F, Baaden M, Delarue M, Corringer PJ. A locally closed conformation of a bacterial pentameric proton-gated ion channel. Nat. Struct. Mol. Biol.. 2012
32. Thompson AJ, Lummis SC. A single ring of charged amino acids at one end of the pore can control ion selectivity in the 5-HT3 receptor. Br. J. Pharmacol. 2003; 140:359–365. [PubMed: 12970096]
33. Keramidas A, Moorhouse AJ, French CR, Schofield PR, Barry PH. M2 pore mutations convert the glycine receptor channel from being anion- to cation-selective. Biophys. J. 2000; 79:247–259. [PubMed: 10866951]
34. Fritsch S, Ivanov I, Wang H, Cheng X. Ion selectivity mechanism in a bacterial pentameric ligand-gated ion channel. Biophys. J. 2011; 100:390–398. [PubMed: 21244835]
35. Gonzalez-Gutierrez G, Lukk T, Agarwal V, Papke D, Nair SK, Grosman C. Mutations that stabilize the open state of the Erwinia chrisanthemi ligand-gated ion channel fail to change the conformation of the pore domain in crystals. Proc. Natl. Acad. Sci. U. S. A. 2012; 109:6331–6336. [PubMed: 22474383]
36. Erkkila BE, Weiss DS, Wotring VE. Picrotoxin-mediated antagonism of alpha3beta4 and alpha7 acetylcholine receptors. Neuroreport. 2004; 15:1969–1973. [PubMed: 15305147]
37. Pribilla I, Takagi T, Langosch D, Bormann J, Betz H. The atypical M2 segment of the beta subunit confers picrotoxinin resistance to inhibitory glycine receptor channels. EMBO J. 1992; 11:4305–4311. [PubMed: 1385113]
38. Takeuchi A, Takeuchi N. A study of the action of picrotoxin on the inhibitory neuromuscular junction of the crayfish. J. Physiol. 1969; 205:377–391. [PubMed: 5357245]
39. Wang TL, Hackam AS, Guggino WB, Cutting GR. A single amino acid in gamma-aminobutyric acid rho. 1 receptors affects competitive and noncompetitive components of picrotoxin inhibition. Proc. Natl. Acad. Sci. U. S. A. 1995; 92:11751–11755. [PubMed: 8524842]

40. Duret G, Van Renterghem C, Weng Y, Prevost M, Moraga-Cid G, Huon C, Sonner JM, Corringer PJ. Functional prokaryotic-eukaryotic chimera from the pentameric ligand-gated ion channel family. Proc. Natl. Acad. Sci. U. S. A.. 2011

41. Das P, Dillon GH. Molecular determinants of picrotoxin inhibition of 5-hydroxytryptamine type. 3 receptors. J. Pharmacol. Exp. Ther. 2005; 314:320–328. [PubMed: 15814570]

42. Violet JM, Downie DL, Nakisa RC, Lieb WR, Franks NP. Differential sensitivities of mammalian neuronal and muscle nicotinic acetylcholine receptors to general anesthetics. Anesthesiology. 1997; 86:866–874. [PubMed: 9105231]

43. Flood P, Ramirez-Latorre J, Role L. Alpha 4 beta 2 neuronal nicotinic acetylcholine receptors in the central nervous system are inhibited by isoflurane and propofol, but alpha 7-type nicotinic acetylcholine receptors are unaffected. Anesthesiology. 1997; 86:859–865. [PubMed: 9105230]

44. Pistis M, Belelli D, Peters JA, Lambert JJ. The interaction of general anaesthetics with recombinant GABAA and glycine receptors expressed in Xenopus laevis oocytes: a comparative study. Br. J. Pharmacol. 1997; 122:1707–1719. [PubMed: 9422818]

45. Wang HL, Cheng X, Taylor P, McCammon JA, Sine SM. Control of cation permeation through the nicotinic receptor channel. PLoS Comput. Biol. 2008; 4:e41. [PubMed: 18282090]

46. Chen Q, Cheng MH, Xu Y, Tang P. Anesthetic binding in a pentameric ligand-gated ion channel: GLIC. Biophys. J. 2010; 99:1801–1809. [PubMed: 20858424]

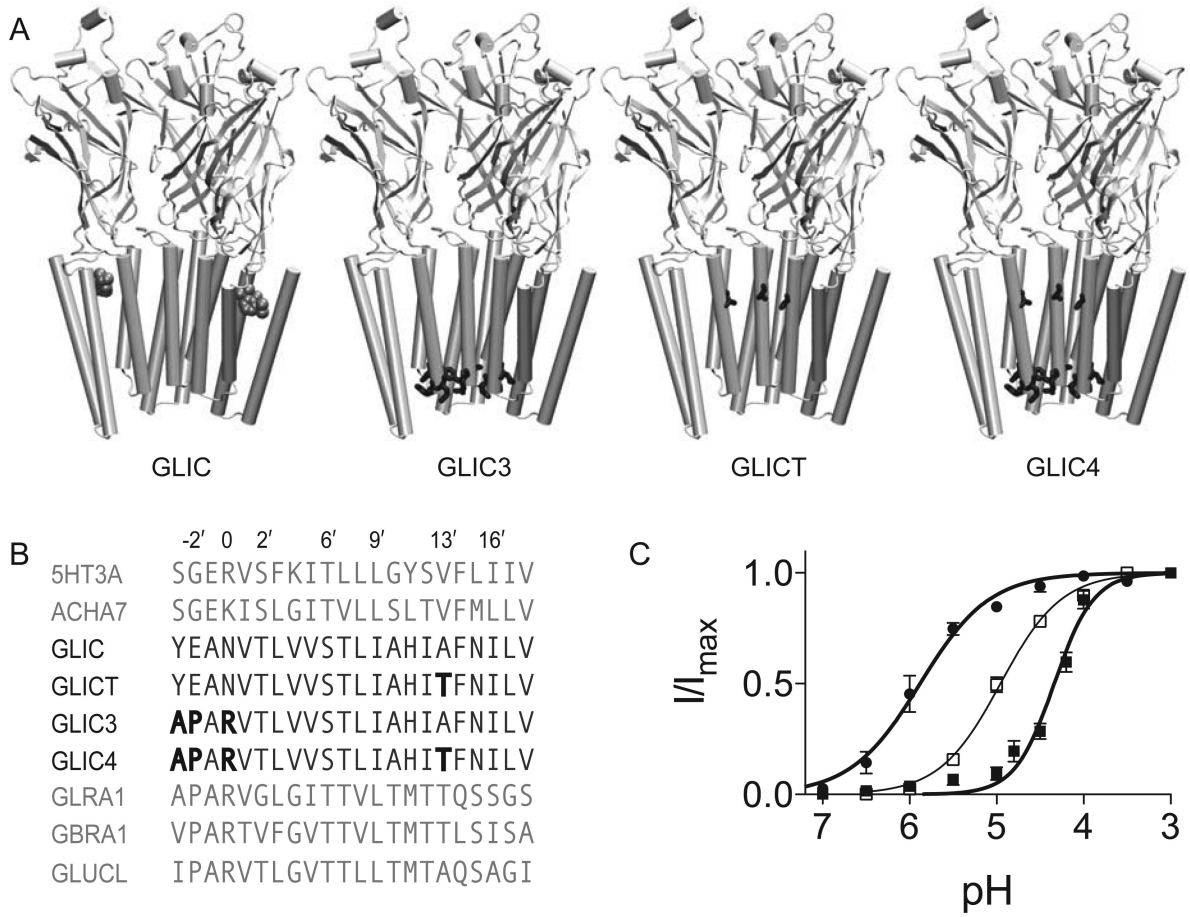

Figure 1. Mutagenesis of GLIC

(**A**) View of GLIC and the indicated mutant constructs in the plane of the membrane with the front two subunits removed to show the interior of the pore. Propofol is shown in space-filling representation at its binding site. The residues with the following mutations are indicated in their respective constructs: Y–3′A, E–2′P, N0′R and A13′T (**B**) Alignment of GLIC with select members of the pLGIC family with the mutations in GLIC3, GLICT and GLIC4 indicated in bold. Pore facing residues are numbered. The sequences above the GLIC constructs are cation channels; the sequences below are anion channels. (**C**) pH response curves for GLIC4 (■) and GLICT (●). The pH corresponding to the EC_{50} was 5.9 and 4.3 for GLICT and GLIC4, respectively. The data are fit to the Hill equation. Error bars represent standard error, n=7 oocytes.

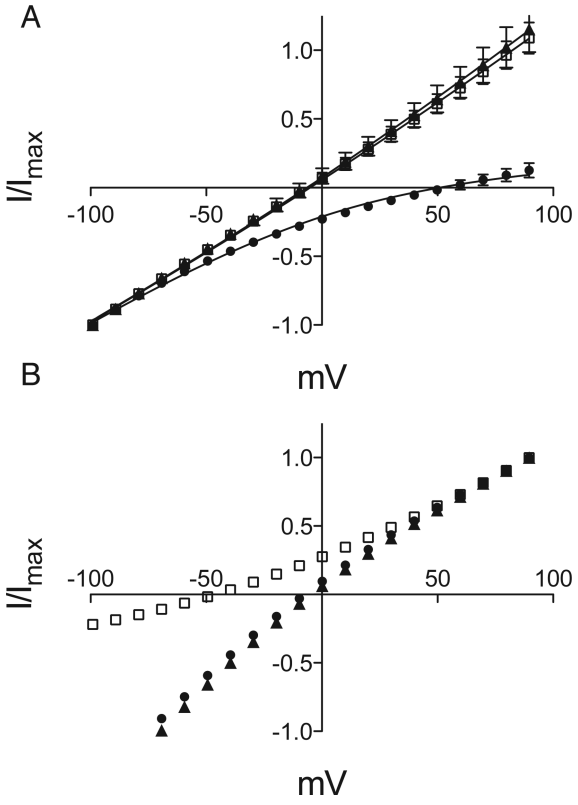

Figure 2. GLIC4 is selective for Cl^-

(**A**) Asymmetric IV curves for GLIC4 with 130 mM NaCl (▲), choline chloride (▱) or sodium gluconate (●) in the external solution. Error bars represent standard error, n=5. The 60 mV positive shift in reversal potential on replacement of chloride with gluconate is indicative of chloride selectivity. Permeability ratios were obtained from global nonlinear regression to the Goldman-Hodgkin-Katz equation (solid lines). (**B**) Asymmetric IV curves for GLICT. The legend is the same as for (**A**). Error bars (smaller than the symbol size) represent standard error, n=5. The 45 mV negative shift in reversal potential on replacement of sodium with choline is indicative of sodium selectivity.

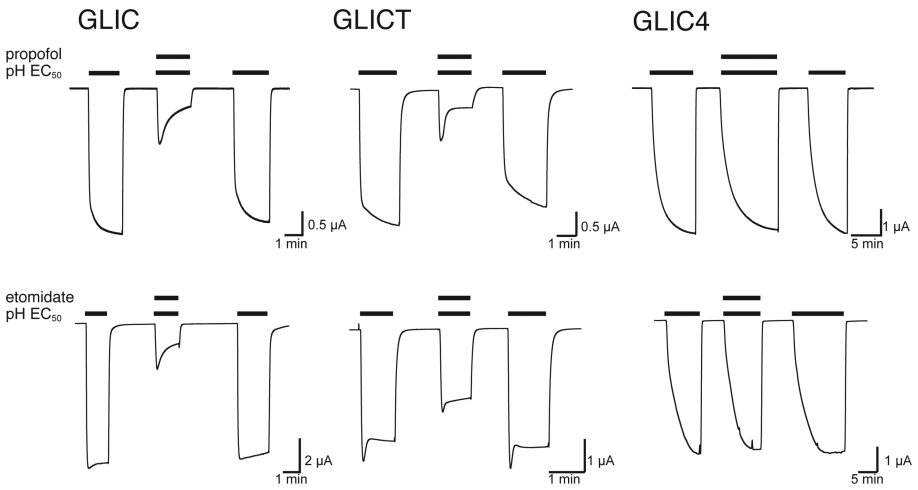

Figure 3. GLIC4 is insensitive to anesthetics

Representative traces of inhibition by the indicated anesthetics. Anesthetics were applied at the pH corresponding to the EC_{50} for each construct: GLIC pH 5, GLICT pH 5.9 and GLIC4 pH 4.3. Anesthetic concentrations were 100 µM propofol and 500 µM etomidate.

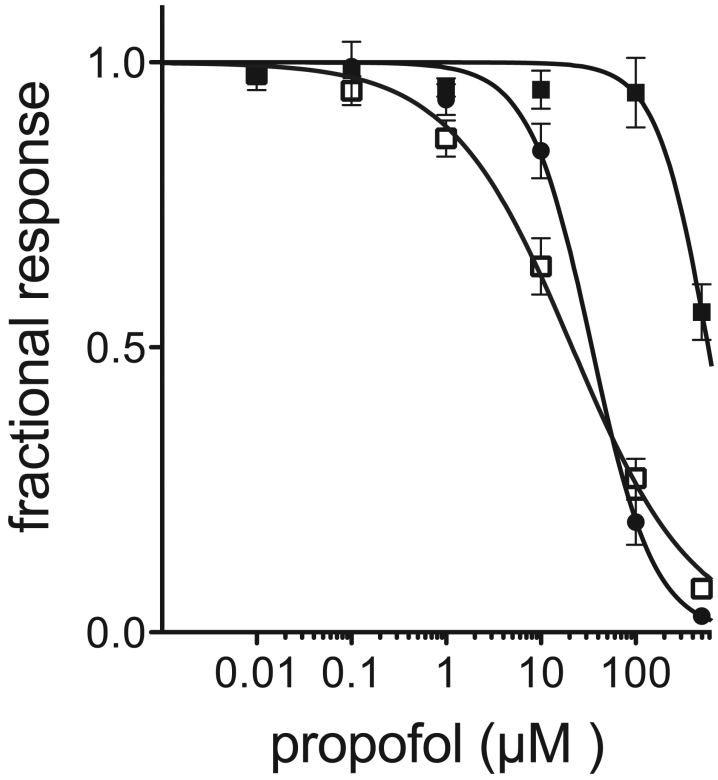

Figure 4. Propofol inhibition of GLIC (▱), GLICT (●) and GLIC4 (■)

Fractional current is plotted as a function of propofol concentration at the pH corresponding to the EC_{20} for the pH activation of each construct. Error bars represent standard error, n=5. IC_{50} for propofol inhibition are 21, 35 and 584 μM for for GLIC, GLICT and GLIC4, respectively.

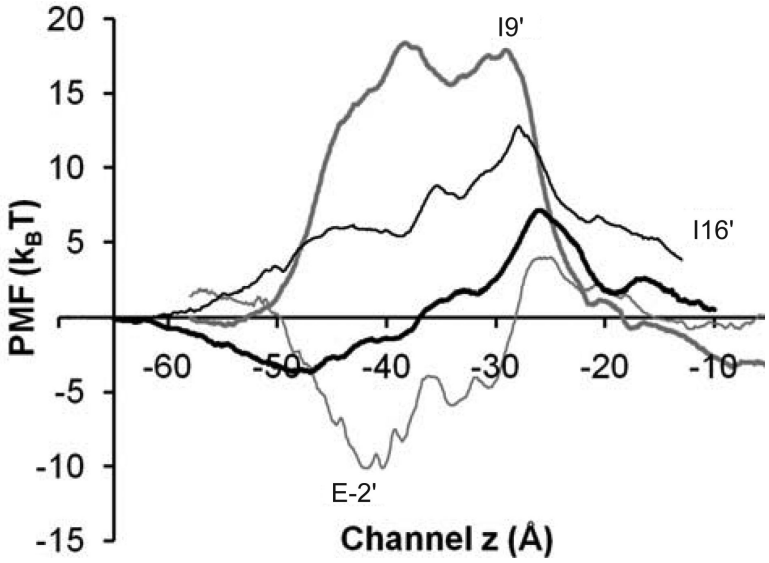

Figure 5. Comparison of MD−calculated single ion PMFs

Single ion PMFs for transporting Cl^- or Na^+ ion along the channel centerline. For GLIC4, Cl^- (thick black line), Na^+ (thin black lines); for wild type GLIC, Cl^- (thick gray line), Na^+ (thin gray lines). Residues in GLIC are marked in the figure.

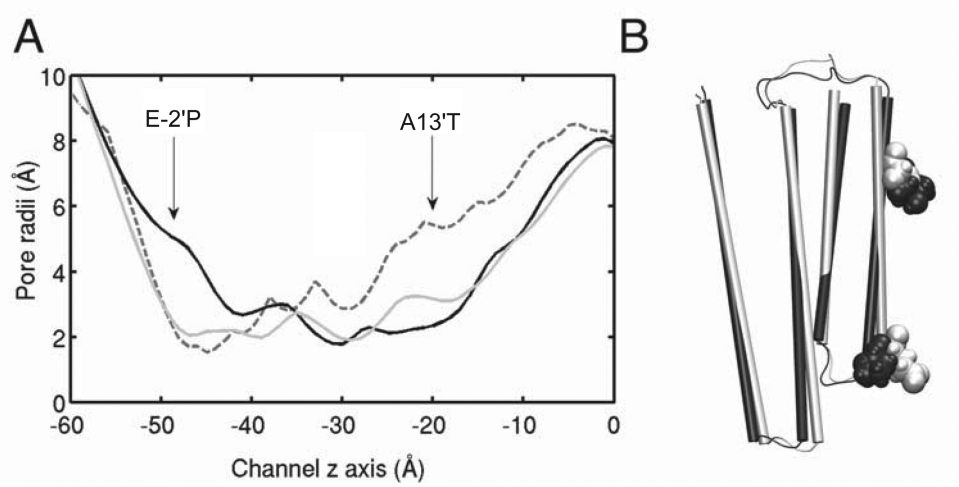

Figure 6. Changes in the GLIC4 pore

(**A**) Comparison of the pore radii of the X-ray structure of GLIC (gray dashed line), the MD equilibrated structures of GLIC (gray solid line) and GLIC4 (black solid line) after simulations for 50 ns. Simulation results were averaged based on 100 snapshots near 50 ns and from three replicate runs. The standard deviation of the averaged pore radii in the TM domain is within 0.3 Å. (**B**) Alignment of a representative equilibrated GLIC (white) with a representative equilibrated GLIC4 (black) after 30 ns simulations. E–2′ in GLIC and E–2′P in GLIC4 are in VDW presentation. For clarity, only the transmembrane domain of one subunit is shown.

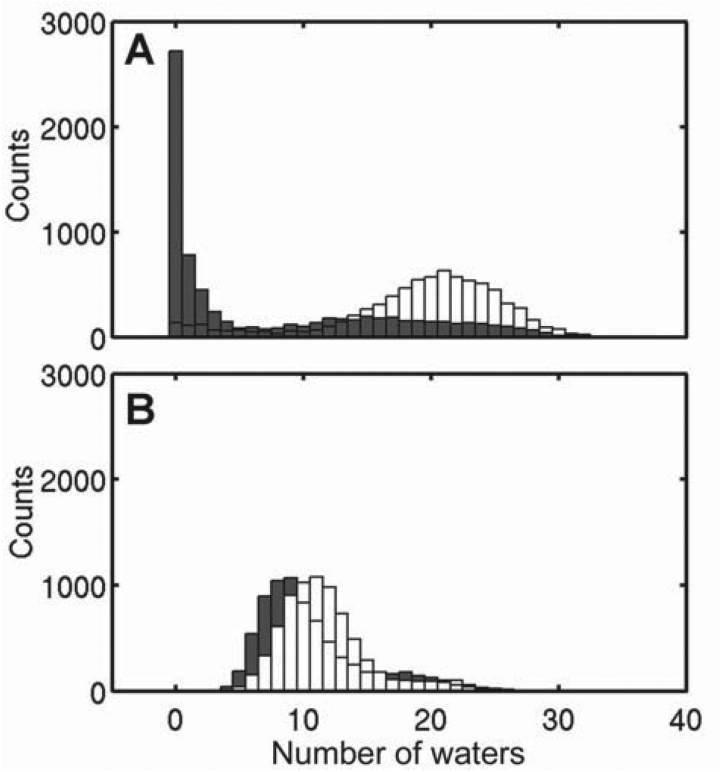

Figure 7. Propofol dehydrates GLIC but not GLIC4

Histograms of number of waters inside the hydrophobic gate region (I9′ to I16′) of (**A**) GLIC (light gray) and GLIC-PFL (black) and (**B**) GLIC4 (light gray) and GLIC4-PFL (black). Snapshots with a 20-picosecond interval were taken from each run. A total of 1400 structures were used for each histogram analysis.